Available online at www.sciencedirect.com
ScienceDirect
Dyes and Pigments 76 (2008) 817–824
DYES and PIGMENTS
www.elsevier.com/locate/dyepig

Photocatalytic degradation of C.I. Basic Violet 10 using TiO_2 catalysts supported by Y zeolite: An investigation of the effects of operational parameters

Cheng-Cai Wang*, Chung-Kung Lee, Meng-Du Lyu, Lain-Chuen Juang

Green Environment R&D Center and Department of Environmental Engineering, Vanung University, Chung-Li, Tao-Yuan 32061, Taiwan, ROC

Received 17 December 2006; received in revised form 11 February 2007; accepted 13 February 2007
Available online 24 February 2007

Abstract

The physical and chemical states of zeolite-supported TiO_2 were evaluated *via* powder X-ray diffraction (XRD), Fourier transform infrared (FTIR) and nitrogen adsorption–desorption isotherms. The effects of operational parameters, including TiO_2 content, calcination temperature, pH, initial dye concentration, as well as catalyst dosage, on photocatalytic degradation performance were examined. The photocatalytic reaction followed first-order kinetics for all catalysts; optimum photodegradation efficiency was found to result from the use of a high TiO_2 concentration (20% TiO_2), a calcination temperature of 600 °C, alkaline pH (9–10) and a catalyst dosage of 5333 ppm.

Keywords: TiO_2; Y zeolite; Photocatalytic degradation; Cationic dye; Operational parameters; Catalyst

1. Introduction

In our modern industrial society, dyes are widely used in textiles, printing, dyeing, and food. Dye pollutants from these industries are sources of severe environmental contamination [1–3]; indeed, the colour produced by minute amounts of dyes in water are considered to pose a very serious problem because they have a considerable effect on the water environment and are visually unpleasant. Moreover, some dyes are toxic and mostly non-biodegradable and are also harmful to aquatic life. Therefore, the decolorizing of dye wastewater has become a major environmental control problem and there have been many investigations of physical, chemical and biological methods of removing colour from dye wastewater [4–6]. However, in terms of treating dye wastewater, biological processes are ineffective, coagulation and adsorption processes merely transfer the dye pollutants from one phase to another, generating a new and different kind of pollution and necessitating further treatment [7,8]. Recently, photocatalytic degradation using the non-toxic, inexpensive and highly reactive nature of TiO_2 under UV irradiation has been adopted to oxidize dyes in wastewater [9].

Most studies of photocatalytic degradation using TiO_2 have been carried out using suspensions of powdered TiO_2 in the polluted solution. However, there are several limitations to using 'bare' TiO_2 in photocatalytic reactors, notable of which is the fact that TiO_2 aggregates rapidly in suspension, resulting in smaller effective surface area and lower catalytic efficiency. The small size of TiO_2 particles complicates the filtration of suspensions, making slurry photocatalytic reactors impractical. Moreover, owing to its polar surface, the pollutant-adsorbing ability of TiO_2 often appears to be low [10], especially for non-polar, organic compounds [11].

In contrast, as immobilization and pre-concentration of the pollutant substrate on the surface where photons are adsorbed is a desirable feature for effective photodegradation, attempts have been made to immobilize the TiO_2 catalyst on a support, such as ceramic [12], silica [13,14], activated carbon [15,16],

* Corresponding author. Tel.: +886 34515811 716; fax: +886 34622232.
E-mail address: ericwang@msa.vnu.edu.tw (C.-C. Wang).

0143-7208/$ - see front matter © 2007 Elsevier Ltd. All rights reserved.
doi:10.1016/j.dyepig.2007.02.004

clay [17,18], and zeolite [19,20]. Of these, zeolite was found to be an attractive candidate due to its low polar surface and large surface area, as well as its high adsorption capacity for non-polar, organic pollutants. Recently, Zhu et al. [21] have utilized cage-type zeolites (13-X, Na-Y, and 4A) as supports for TiO_2 and showed that these compounds displayed a high degree of photodegradation of degradation of azo dyes in aqueous solution, even at low Ti loading.

This paper concerns the effects of operational parameters on the photoactivity of TiO_2 on a Na-Y zeolite support towards C.I. Basic Violet 10. The physical and chemical states of the zeolite-supported TiO_2 were evaluated using XRD, FTIR spectra and nitrogen adsorption–desorption isotherms under various operational parameters, including TiO_2 content, calcination temperature, pH, initial dye concentration and catalyst dosage.

2. Experimental

2.1. Materials

Powdered particles of Na-Y zeolite (Zeolyst international, Si/Al = 5.1) with a BET surface area of 900 $m^2 g^{-1}$ were used as support for TiO_2. Whilst the pore size of the Na-Y zeolite was not provided by the manufacturer, it was well known that the pore size of Na-Y zeolite is about 0.7–0.74 nm [22,23]. Analytical-grade C.I. Basic Violet 10 (Sigma Chemical Co.) was selected as target organic pollutant; its structure is shown in Fig. 1. Analytical-grade tetraethylorthotitanate (Merck), hexane (Merck), and heptane (Merck) were used to prepare the catalysts.

2.2. Synthesis of the catalysts

The catalysts were prepared using an impregnation method in which the Ti-source, tetraethylorthotitanate, was added to Na-Y zeolite that had been suspended in hexane/heptane solvent, at a volumetric ratio of 1:1. The mixture was stirred for 1 h in air to hydrolyze tetraethylorthotitanate and then the solvent was removed by rotary vacuum evaporation. The resultant solid was dried at 100 °C for 30 min and treated at 200–700 °C for 6 h. Catalysts were prepared with different TiO_2 loading contents namely 5, 10, 20, 30, and 50%, respectively.

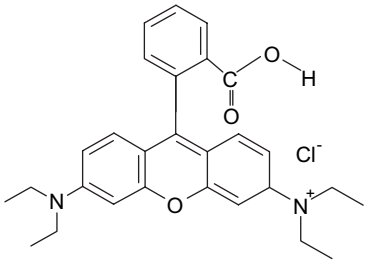

Fig. 1. Chemical structure of C.I. Basic Violet 10.

2.3. Characterization of the catalysts

The catalysts were characterized using different analytical techniques. Their nitrogen adsorption–desorption isotherms were measured at the temperature at which nitrogen liquefied (77 K) using a *Micromeritics TriStar 3000*. The sample (0.1 g) was de-gassed with He for 16 h at 105 °C prior to the adsorption measurement. The specific surface area was determined using a multi-point BET plot and the pore volume was determined by means of a BJH desorption isotherm. The XRD patterns of the catalysts were obtained using a *Thermal ARL* X-ray diffractometer equipped with a CuKα radiation source and graphite monochromator. FTIR spectra were obtained in KBr pellets using a Perkin–Elmer *Model 1600* FTIR spectrophotometer over the range of 4000–400 cm^{-1}.

2.4. Photocatalytic activity measurement

The photocatalytic degradation of C.I. Basic Violet 10 in suspension with the catalyst was performed in a 300 mL reactor. The irradiation source was an *FL-15BL* (TFL, Taiwan) 15 W low-pressure fluorescent lamp with the major fraction of irradiation occurring at 365 nm. The relative photocatalytic activities of the catalysts were evaluated by measuring the loss of dye from the aqueous medium. Prior to illumination, a suspension containing 0.1 g of catalyst and 300 mL of C.I. Basic Violet 10 was stirred continuously in the dark for 1 h. The change in dye concentration after 1 h was used to evaluate the degree of its adsorption on the photocatalyst. The concentration of the dye in bulk solution at this point was used as the initial concentration for the kinetic treatment of the photodegradation process. At regular time intervals of illumination, a sample of the mixture was collected, centrifuged and filtered through a *Millipore* filter (pore size 0.45 μm). The concentration of C.I. Basic Violet 10 was measured using a Shimadzu *UV-160A*, UV–vis spectrophotometer at 554 nm, the λ_{max} of C.I. Basic Violet 10. The photodegradation efficiency (X) was given by Eq. (1)

$$X = \frac{C_0 - C}{C_0}, \tag{1}$$

where C_0 was the initial dye concentration and C was the concentration of C.I. Basic Violet 10 at time t. For all photocatalytic experiments, measurements were conducted at least twice and the average value was recorded. The standard errors in the photodegradation efficiency for all photocatalytic experiments were <0.02.

3. Results and discussion

3.1. Characterization of TiO_2/zeolite catalysts

3.1.1. XRD analysis

X-ray powder diffraction was used to assess the crystallinity of the catalyst particles. The XRD patterns of catalysts of differing TiO_2 loading contents are shown in Fig. 2 from

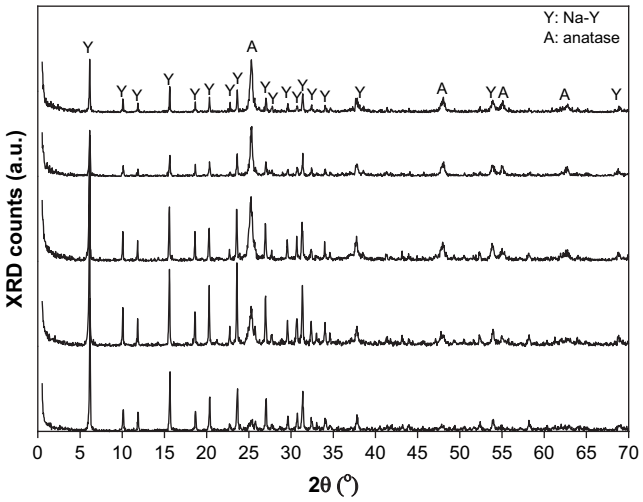

Fig. 2. XRD patterns of TiO_2 supported by Y zeolite with different loading contents; from bottom to top: 5, 10, 20, 30, and 50 wt.% TiO_2 loading, respectively. Condition: calcination temperature = 600 °C.

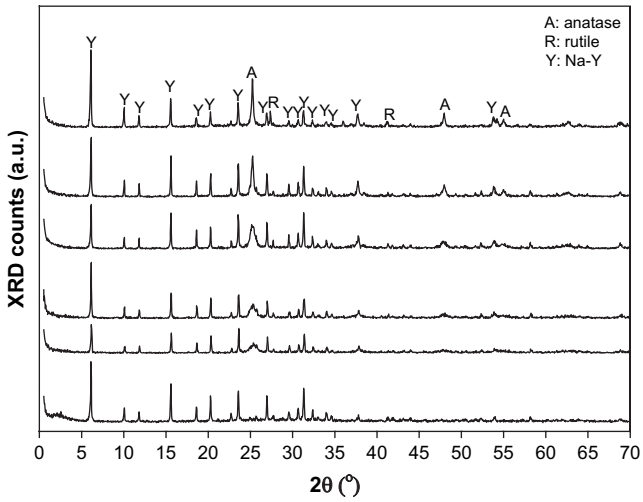

Fig. 3. The dependence of the XRD patterns of catalyst (20 wt.% TiO_2) on the calcination temperature; from bottom to top: 200, 300, 400, 500, 600, and 700 °C, respectively.

which the characteristic XRD peak of the anatase phase was apparent at $2\theta = 25.4°$ [24] for all catalysts; peaks corresponding to the anatase phase also appeared at $2\theta = 48.3$ and 54.9°. No significant peak of the rutile phase was observed at $2\theta = 27.4°$. As expected, with increased TiO_2 loading, sharper peaks were observed due to the increased crystalline quality of TiO_2. In the cases of catalysts with low TiO_2 loading, the small amount of well-dispersed TiO_2 on the Y zeolite inhibited the mutual approach of fine TiO_2 particles, hence leading to the formation of crystals of finer size. However, it is probable that with increase in TiO_2 loading, the TiO_2 particle size became larger due to aggregation of TiO_2 particles on the surface of zeolite. The TiO_2 particle size, S, calculated by means of Scherrer's equation ($S = K\lambda/(\beta \cos \theta)$, where K is related to the shape of the polycrystals (0.9), λ, the X-ray wavelength (0.154 nm), β, the full-width at half the maximum of the respective diffraction peak and θ is the Bragg angle), were 8.3, 9.0, 22.1, 28.4, and 28.9 nm for the TiO_2 loadings of 5, 10, 20, 30, and 50 wt.%, respectively. The results as a whole indicate that the TiO_2 particle size increased with increasing TiO_2 loading, possibly due to aggregation of the TiO_2 particles on the surface of the zeolite.

The effects of calcination temperature on the XRD patterns of the TiO_2/zeolite photocatalysts are shown in Fig. 3. At 200 °C, while the characteristic peaks of the anatase and the rutile phase were not observed, anatase crystallite was present on the catalyst at higher calcination temperature (≥300 °C) and the rutile crystallite was not observed until 700 °C. The low intensity and broad peak character of the XRD spectra of the catalysts at low calcination temperatures indicate that highly dispersed, fine particles of anatase TiO_2 were formed on the Y zeolite support. The relatively larger TiO_2 crystallites formed at high temperature (600 and 700 °C) were evidenced by sharper TiO_2 peaks. The size of the TiO_2 particles calculated by means of Scherrer's equation were 7.6, 7.9, 10.5, 28.4, and 33.1 nm for 300, 400, 500, 600 and 700 °C, respectively.

3.1.2. FTIR spectra

In this work, the TiO_2 was deposited on the surface of the zeolites rather than the Ti being incorporated into the silica framework. As shown in Fig. 4, since no band around 960 cm^{-1} was found for any of the catalysts, the replacement of the tetrahedral Si sites with Ti during preparation did not take place [25].

3.1.3. BET surface area, pore volume, and pore size distribution

The pore volume and specific surface area of catalysts with different TiO_2 loading were determined using nitrogen adsorption–desorption isotherms. In all cases, both the pore volume and the surface area of the catalysts decreased with increasing loading of TiO_2, as shown in Fig. 5. The observed reductions in pore volume and surface area indicated that the TiO_2/zeolite was not simply a mechanical mixture but, rather, resulted from

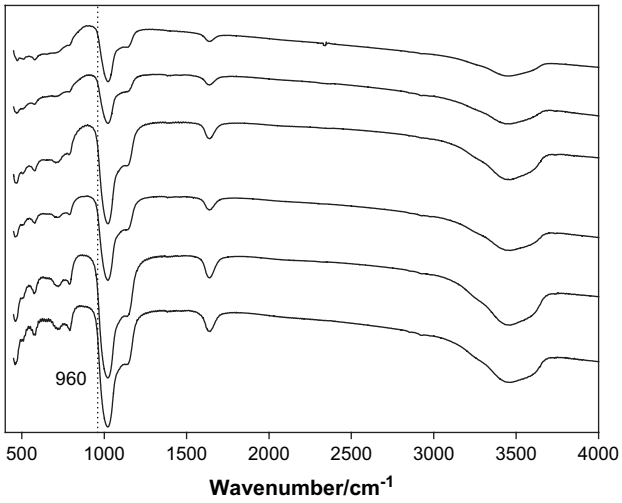

Fig. 4. FTIR patterns of TiO_2 supported by Y zeolite with different loading contents; from bottom to top: Na-Y zeolite, 5, 10, 20, 30, and 50 wt.% TiO_2 loading, respectively. Condition: calcination temperature = 600 °C.

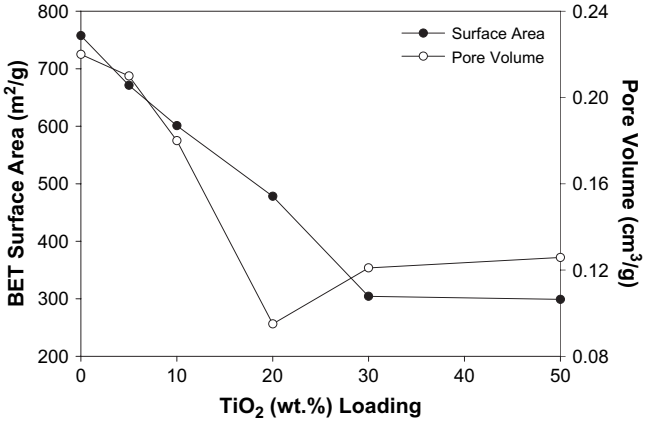

Fig. 5. Both BET surface area (●) and pore volume (○) of catalysts versus TiO_2 loading on zeolite. Condition: calcination temperature = 600 °C.

the fact that TiO_2 was dispersed on the zeolite surfaces and the pores of zeolite were partially blocked with TiO_2. As the pore size of Na-Y zeolite was smaller than the size of the TiO_2 particles supported by the zeolite, the particles might not be deposited inside the pores of zeolite. Moreover, at high TiO_2 loading, the TiO_2 particles will likely have aggregated on the surface of zeolite and, if voids in this aggregation developed, additional pore volume might be created. As seen from the corresponding pore size distributions of the above-examined samples (Fig. 6), additional pore size (<20 nm) was observed for samples with 30 and 50% TiO_2, which can be attributed to voids in the aggregation of the TiO_2 particles. This result might induce a slight increase in the pore volume, as shown in Fig. 5.

3.2. Batch photocatalytic degradation study

3.2.1. Adsorption of C.I. Basic Violet 10 on the TiO_2/zeolite catalysts

It is generally accepted that adsorption is critical in heterogeneous photocatalytic oxidation processes [26]. However, in this study, dark adsorption experiments under different conditions that included different TiO_2 content, calcination temperature, pH, initial dye concentration and catalyst dosage revealed that there was no obvious adsorption of C.I. Basic Violet 10 on the catalysts (the adsorptive removal efficiency was <0.1 as shown in Figs. 7 and 8). It can be proffered that dye adsorption may not be the most important factor for photocatalytic degradation activity of the used catalysts in this work. As the maximum diameter of C.I. Basic Violet 10 (>1 nm) was larger than the aperture size of Na-Y zeolite (<1 nm), the dye would not be able to move into the large inner surfaces of the zeolite so that the majority of the adsorptive ability of zeolite could not be utilized. Hence, the dye molecules could only be adsorbed on the outer surface of the zeolite and TiO_2; at the same time, steric hindrance between the large dye molecules may well have hampered the approach of other dye molecules to the surface of the catalyst. Thus, no obvious dye adsorption could be observed and, therefore, owing to the fact that the dye was not adsorbed significantly onto the catalyst, most of the photocatalytic reaction did not take place on the photocatalyst surface and, instead, proceeded *via* reaction of the dye with hydroxyl radicals generated after the adsorption of hydroxyl ions onto the catalyst surface and followed by reactions with holes in the excited, semiconductive catalyst [27].

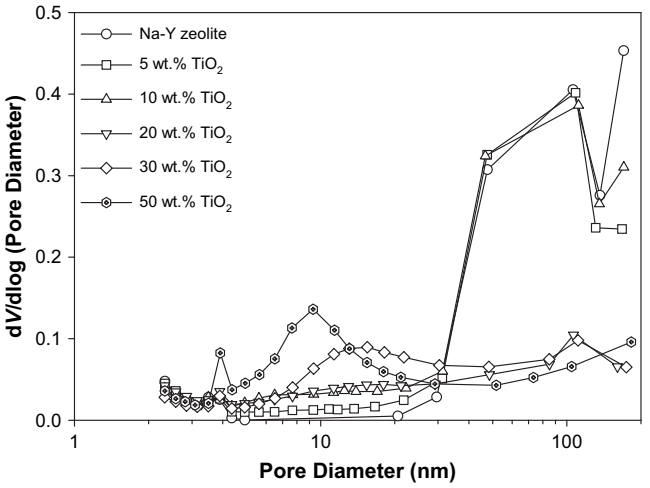

Fig. 6. Pore size distributions of catalyst with different TiO_2 loading contents, where V was cumulative pore volume.

3.2.2. Effect of TiO_2 content

The effects of TiO_2 content on the performance of the TiO_2/zeolite catalysts in the photodegradation of C.I. Basic Violet 10 are shown in Fig. 7 from which it is evident that the decolorization rates did not increase linearly with increasing TiO_2 content. Indeed, maximum value was achieved at a medium loading of 20% TiO_2 which might be due to two competitive processes [21]. In general, the greater the amount of TiO_2, the higher the reaction rates should be, due to the fact that

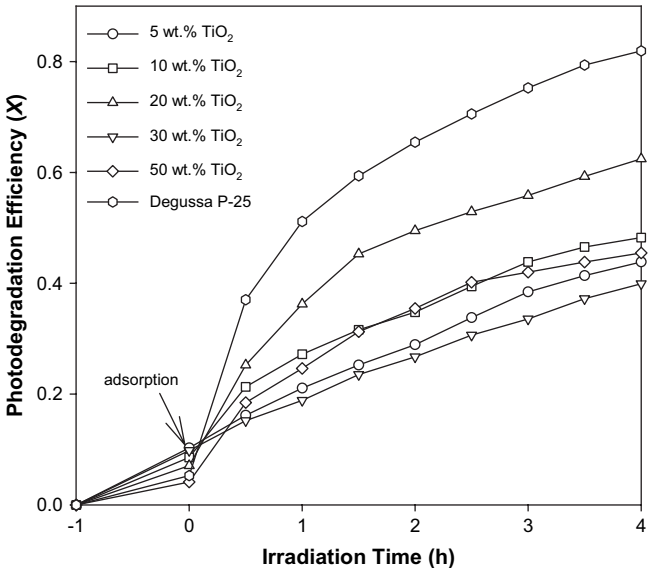

Fig. 7. Effect of TiO_2 loading on photodegradation efficiency of catalyst. Conditions: calcination temperature = 600 °C, pH = 5, catalyst dosage = 333 ppm, and initial dye concentration = 50 ppm.

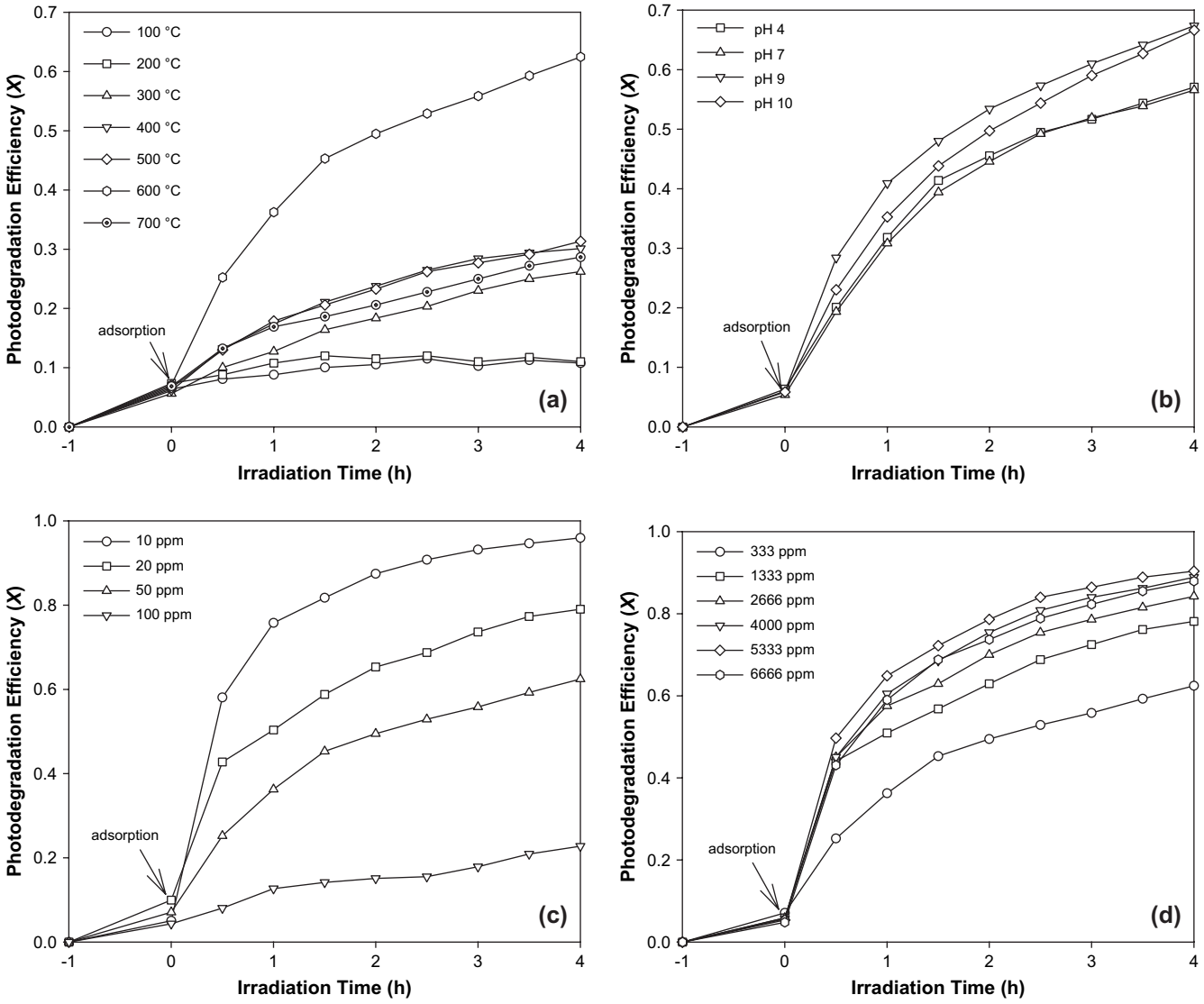

Fig. 8. (a) Effect of calcination temperature on the photodegradation efficiency of catalyst. Conditions: TiO_2 loading = 20 wt.%, pH = 5, catalyst dosage = 333 ppm, and initial dye concentration = 50 ppm. (b) Effect of pH on the photodegradation efficiency of catalyst. Conditions: TiO_2 loading = 20 wt.%, calcination temperature = 600 °C, catalyst dosage = 333 ppm, and initial dye concentration = 50 ppm. (c) Effect of initial dye concentration on the photodegradation efficiency of catalyst. Conditions: TiO_2 loading = 20 wt.%, calcination temperature = 600 °C, pH = 5, and catalyst dosage = 333 ppm. (d) Effect of catalyst dosage on the photodegradation efficiency. Conditions: TiO_2 loading = 20 wt.%, calcination temperature = 600 °C, pH = 5, and initial dye concentration = 50 ppm.

more holes and hydroxyl radicals were generated. However, more TiO_2 would also induce greater aggregation of the TiO_2 particles at the surface of the zeolite, with the effect that the TiO_2 particle size increased and the specific surface area of TiO_2 decreased, leading to a reduction in reaction rate. Moreover, it should be noted that because adsorption of the dye onto the catalysts was insignificant in this system, the effects of the reduced surface area and lower pore volume of the catalysts (induced by the TiO_2 on the zeolites) on photocatalytic rate (or the adsorption of the dye) will be slight. Therefore, the factor that caused the observed sharp decrease in photocatalytic efficiency at 30 and 50% TiO_2 loading is aggregation of the TiO_2 particles.

The performance of a commercial titanium dioxide *P25* (Degussa AG, Germany) is given in the Fig. 7 for comparison. The photocatalytic efficiency of all TiO_2/zeolite samples was lower than that of P25, which is well known to be an excellent, commercial pure TiO_2 photocatalyst. Since aggregation of the TiO_2 particles played a key role in the decreased photocatalytic activity of the TiO_2/zeolite composite materials at high TiO_2 loading, it was difficult for the TiO_2/zeolite catalyst to surpass that of a pure TiO_2 catalyst.

3.2.3. Effect of calcination temperature

As mentioned in the XRD analysis, higher calcination temperatures might cause large TiO_2 crystallites to form on the surface of the zeolite support. Therefore, it is to be expected that catalysts treated at higher calcination temperature might display better photocatalytic degradation performance. As shown in Fig. 8(a), photodegradation efficiency increased with increasing calcination temperature and optimum temperature was found to be 600 °C. The sharp decrease in

photocatalytic degradation rate for the catalyst treated at 700 °C may have two causes: one is overgrowth of the TiO_2 crystallite size and the other the existence of a rutile phase in the TiO_2 crystal. As mentioned previously, the TiO_2 particle sizes were 7.6, 7.9, 10.5, 28.4, and 33.1 nm for calcination temperatures of 300, 400, 500, 600 and 700 °C, respectively. On the other hand, a clear rutile peak was observed at $2\theta = 27.4°$ for catalysts heat-treated at 700 °C; this was not found at other temperatures, as shown in Fig. 3. As the particle size of TiO_2 treated at 700 °C was similar to that of the 600 °C sample, it can be concluded that the low photocatalytic degradation rate of the catalyst treated at 700 °C can be attributed to the existence of a rutile phase in the TiO_2 crystal.

3.2.4. Effect of pH

It is well known that pH influences the rate of photocatalytic degradation of some organic compounds [28]; it was also an important operational variable in practical wastewater. Fig. 8(b) shows the photodegradation of C.I. Basic Violet 10 as a function of pH in the range 4–10, from which it is clear that best results were obtained in alkaline solution (pH 9–10). Based on the zero point of the TiO_2 charge, the surface was presumably positively charged in acidic solution and negatively charged in alkaline solution [29]. Thus, it is reasonable to expect that the electrical charge of the dye and the photocatalyst surface will determine the extent of adsorption. C.I. Basic Violet 10 comprises organic cations and inorganic anions in solution; in alkaline solution, attractive forces between the dye cation and the photocatalyst surface would favour adsorption and so photodegradation efficiency will be favoured by high pH.

In contrast, at low pH the photocatalyst's surface will be positively charged and repulsive forces between the photocatalyst surface and the cationic dye will lead to a decrease in both dye adsorption and photodegradation efficiency. As shown in Fig. 8(b), however, the adsorption of the dye onto the catalyst was similar at all pH values; importantly, the extent of this adsorption was low, indicating that the major photocatalytic reaction did not take place on the photocatalyst surface but, instead, proceeds *via* reaction of the dye with hydroxyl radicals. Therefore, a possible reason for the behavior seen in Fig. 8(b) is that the alkaline pH range favoured the formation of more OH radicals due to the presence of a large quantity of hydroxide ions in the alkaline medium, which enhanced the photocatalytic degradation of the dye significantly. It is also noteworthy that in alkaline solution, whilst the repulsion of hydroxide ions by the negatively charged catalyst surface could lead to a reduction in OH radical formation and, thence, a decrease in photodegradation efficiency, this effect might be insignificant due to the weak effects of pH on the adsorption of ions onto the catalyst.

3.2.5. Effect of initial dye concentration

The effect of the initial dye concentration on photodegradation efficiency is shown in Fig. 8(c). The photodegradation conversion of the dye decreased with increase in initial dye concentration because, as the initial concentration of dye increased, more dye molecules were adsorbed on the surface of the catalyst, and the generation of OH radicals at the catalyst surface was reduced since the active sites were occupied by dye cations. Moreover, as the concentration of dye increased, this also caused the dye molecules to adsorb light with the result that fewer photons could reach the photocatalyst surface and so, photodegradation efficiency decreased [30,31].

3.2.6. Effect of catalyst dosage

The effect of the amount of catalyst on dye photodegradation efficiency is shown in Fig. 8(d). It can be seen that, with an increase in catalyst dosage, the decolorization rate increased due to an increase in active sites. The decolorization rate achieved a maximum at a dosage of 5333 ppm and then decreased with increase in catalyst dosage. This might be due to the scattering of light and reduction in light penetration through the solution brought about as a result of an excess of catalyst particles [32]. In addition, the agglomeration and sedimentation of the catalyst particles at high dosage might also have a negative effect on the decolorization rate.

3.2.7. Kinetics of the photocatalytic degradation of C.I. Basic Violet 10

In general, the dependency of photocatalytic reaction rates on the concentration of organic pollutants is well described by the Langmuir–Hinshelwood kinetic model [33]:

$$r = \frac{dC}{dt} = \frac{kKC}{1 + KC}. \tag{2}$$

The above equation can be simplified to a pseudo-first-order equation

$$\ln\left(\frac{C_0}{C}\right) = kKt = k't, \tag{3}$$

where r is the oxidation rate of the reactant (mg/L h^{-1}), C_0 the initial concentration of the reactant (mg/L), C the concentration of the reactant at time t (mg/L), t the illumination time, k the reaction rate constant (h^{-1}), and K is the adsorption coefficient of the reactant onto the catalyst particles (L/mg).

In order to examine whether the reaction rate could be congruent with a first-order reaction under different conditions, a $\ln(C/C_0)$ versus reaction time, t, was plotted (Fig. 9) for different TiO_2 loadings. As shown in Fig. 9, a good linear relationship existed between the $\ln(C/C_0)$ versus t at the initial reaction stage, indicating that Eq. (3) represents the photocatalytic rate of the dye. The calculated apparent rate constants for catalysts with a TiO_2 loading of 5, 10, 20, 30, and 50% were 0.119 ($R^2 = 0.9973$), 0.190 ($R^2 = 0.9932$), 0.347 ($R^2 = 0.9851$), 0.103 ($R^2 = 0.9989$), and 0.185 ($R^2 = 0.9847$) h^{-1}, respectively. As shown by the reaction rate constants, the photodegradation rate increased with increasing TiO_2 loading and reached a maximum value at 20% TiO_2.

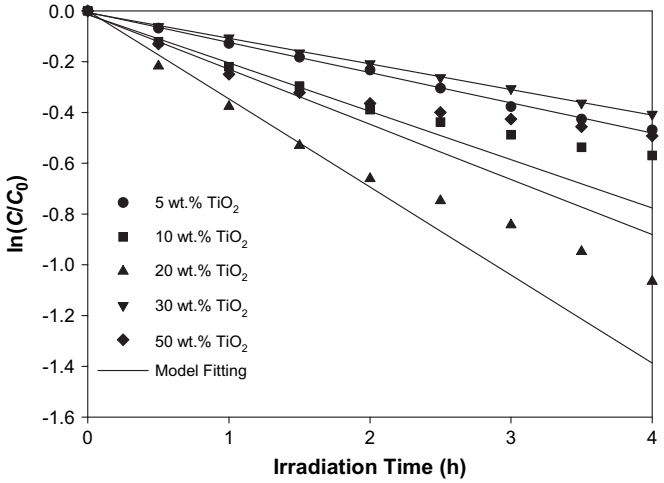

Fig. 9. Relationship between $\ln(C/C_0)$ and irradiation time for kinetic data shown in Fig. 7.

4. Conclusions

Higher TiO_2 loadings and calcination temperatures may well produce larger TiO_2 crystallites on the zeolite support. Moreover, there was found to be no replacement of the tetrahedral Si sites with Ti during preparation. The TiO_2/zeolite composite catalyst was not simply a mechanical mixture but, rather, TiO_2 was dispersed on the support and the pores of zeolite were partially blocked. The major reactions did not take place on the photocatalyst surface and instead proceed *via* reaction of the dye with hydroxyl radicals, because the dye was not adsorbed significantly on the catalyst. TiO_2 supported by the Na-Y zeolite could be used to efficiently degrade the basic dye. The photocatalytic reaction followed first-order kinetics and a high TiO_2 content (20%), high calcination temperature (600 °C), alkaline pH (9–10) and a catalyst dosage of 5333 ppm, as well as a small initial dye concentration (10 ppm), yields optimum photocatalytic degradation performance.

References

[1] Pokhrel D, Viraraghavan T. Treatment of pulp and paper mill wastewater – a review. Science of the Total Environment 2004;333:37–58.
[2] Tünay O, Kabdasli I, Eremektar G, Orhon D. Color removal from textile wastewaters. Water Science and Technology 1996;34:9–16.
[3] Cassano A, Molinari R, Romano M, Drioli E. Treatment of aqueous effluents of the leather industry by membrane processes: a review. Journal of Membrane Science 2001;181:111–26.
[4] Hu C, Yu JC, Hao Z, Wong PK. Photocatalytic degradation of triazine-containing azo dyes in aqueous TiO_2 suspensions. Applied Catalysis B: Environmental 2003;42:47–55.
[5] Wang CC, Juang LC, Lee CK, Hsu TC, Lee JF, Chao HP. Effects of exchanged surfactant cations on the pore structure and adsorption characteristics of montmorillonite. Journal of Colloid and Interface Science 2004;280:27–35.
[6] Lourenco ND, Novais JM, Pinheiro HM. Effect of some operational parameters on textile dye biodegradation in a sequential batch reactor. Journal of Biotechnology 2001;89:163–74.
[7] Slokar YM, Le Marechal AM. Methods of decoloration of textile wastewaters. Dyes and Pigments 1998;37:335–56.
[8] Galindo C, Jacques P, Kalt A. Photooxidation of the phenylazonaphthol AO20 on TiO_2: kinetic and mechanistic investigations. Chemosphere 2001;45:997–1005.
[9] Fox MA, Dulay MT. Heterogeneous photocatalysis. Chemical Reviews 1993;93:341–57.
[10] Torimoto T, Okawa Y, Takeda N, Yoneyama H. Effect of activated carbon content in TiO_2-loaded activated carbon on photodegradation behaviors of dichloromethane. Journal of Photochemistry and Photobiology A: Chemistry 1997;103:153–7.
[11] Lepore GP, Persaud L, Langford CH. Supporting titanium dioxide photocatalysts on silica gel and hydrophobically modified silica gel. Journal of Photochemistry and Photobiology A: Chemistry 1996;98:103–11.
[12] Sunada F, Heller A. Effects of water, salt water, and silicone overcoating of the TiO_2 photocatalyst on the rates and products of photocatalytic oxidation of liquid 3-octanol and 3-octanone. Environmental Science & Technology 1998;32:282–6.
[13] Chen Y, Wang K, Lou L. Photodegradation of dye pollutants on silica gel supported TiO_2 particles under visible light irradiation. Journal of Photochemistry and Photobiology A: Chemistry 2004;163:281–7.
[14] Xu Y, Zheng W, Liu W. Enhanced photocatalytic activity of supported TiO_2: dispersing effect of SiO_2. Journal of Photochemistry and Photobiology A: Chemistry 1999;122:57–60.
[15] Hermann J, Matos J, Disdier J, Guillard C, Laine J, Malato S, Blanco J. Solar photocatalytic degradation of 4-chlorophenol using the synergistic effect between titania and activated carbon in aqueous suspension. Catalysis Today 1999;54:255–65.
[16] Yoneyama H, Torimoto T. Titanium dioxide/adsorbent hybrid photocatalysts for photodestruction of organic substances of dilute concentrations. Catalysis Today 2000;58:133–40.
[17] Ooka C, Yoshida H, Suzuki K, Hattori T. Highly hydrophobic TiO_2 pillared clay for photocatalytic degradation of organic compounds in water. Microporous and Mesoporous Materials 2004;67:143–50.
[18] Sun Z, Chen Y, Ke Q, Yang Y, Yuan J. Photocatalytic degradation of cationic azo dye by TiO_2/bentonite nanocomposite. Journal of Photochemistry and Photobiology A: Chemistry 2002;149:169–74.
[19] Kang MG, Park HS, Kim KJ. Effect of improved crystallinity of titanium silicalite-2 on photodecomposition of simple aromatic hydrocarbons. Journal of Photochemistry and Photobiology A: Chemistry 2002;149:175–81.
[20] Bhattacharyya A, Kawi S, Ray MB. Photocatalytic degradation of orange II by TiO_2 catalysts supported on adsorbents. Catalysis Today 2004;98:431–9.
[21] Zhu C, Wang L, Kong L, Yang X, Wang L, Zheng S, Chen F, MaiZhi F, Zong H. Photocatalytic degradation of AZO dyes by supported TiO_2 + UV in aqueous solution. Chemosphere 2000;41:303–9.
[22] Storck S, Bretinger H, Maier WF. Characterization of micro- and mesoporous solids by physisorption methods and pore size analysis. Applied Catalysis A: General 1998;174:137–46.
[23] Ruthven DM. Principles of adsorption & adsorption processes. New York: John Wiley & Sons; 1984. p. 12.
[24] Liqiang J, Xiaojun S, Weimin C, Zili X, Yaoguo D, Honggang F. The preparation and characterization of nanoparticle TiO_2/Ti films and their photocatalytic activity. The Journal of Physics and Chemistry of Solids 2003;64:615–23.
[25] de Man Andries JM, Sauer J. Coordination, structure, and vibrational spectra of titanium in silicate and zeolites in comparison with related molecules: an ab initio study. The Journal of Physical Chemistry 1996;100:5025–34.
[26] Serpone N, Pelizzetti E. Photocatalysis: fundamentals and applications. New York: Wiley; 1989.
[27] Zielińnska B, Grzechulska J, Kaleńczuk RJ, Morawski AW. The pH influence on photocatalytic decomposition of organic dyes over A11 and P25 titanium dioxide. Applied Catalysis B: Environmental 2003;45: 293–300.
[28] Wu C, Liu X, Wei D, Fan J, Wang L. Photosonochemical degradation of phenol in water. Water Research 2001;35:3927–33.
[29] Fernandez J, Kiwi J, Lizama C, Freer J, Baeza J, Mansilla HD. Factorial experimental design of Orange II photocatalytic discolouration. Journal of Photochemistry and Photobiology A: Chemistry 2002;151:213–9.

[30] Daneshvar N, Salari D, Khataee AR. Photocatalytic degradation of azo dye acid red 14 in water: investigation of the effect of operational parameters. Journal of Photochemistry and Photobiology A: Chemistry 2003;157:111–6.

[31] Grzechulska J, Morawski AW. Photocatalytic decomposition of azo-dye acid black 1 in water over modified titanium dioxide. Applied Catalysis B: Environmental 2002;36:45–51.

[32] Goncalves MST, Oliveira-Campos AMF, Pinto EMMS, Plasencia PMS, Queiroz MJRP. Photochemical treatment of solutions of azo dyes containing TiO_2. Chemosphere 1999;39:781–6.

[33] Turchi CS, Ollis DF. Photocatalytic degradation of organic water contaminants: mechanisms involving hydroxyl radical attack. Journal of Catalysis 1990;122:178–92.